

Evaluation of total suspended matter concentration in wave breaking zone using multispectral satellite images

A.C. Teodoro*^a, A.R.S. Marçal^a, F. V. Gomes^b

^aFaculty of Science, University of Porto, Rua do Campo Alegre, 687, 4169-007 Porto, Portugal

^bFaculty of Engineering, University of Porto, Rua Dr. Roberto Frias, 4200-465 Porto, Portugal

ABSTRACT

Remote sensing techniques are a powerful tool for monitoring littoral zones. Optical sensors can be used to quantify water quality parameters such as suspended sediments. It is possible to estimate the Total Suspended Matter (TSM) concentration using multi-spectral satellite images. In order to extract meaningful information, the satellite data needs to be validated with in situ measurements. The main objective of this work was to quantify the TSM in sea breaking zone, using multi-spectral satellite images. A part of the northwest coast of Portugal, centered around Aveiro, was chosen as a test area. Several methodologies have been used to establish a relationship between the above sea water reflectance and the TSM concentration. Various field trips were done in order to simultaneously obtain water samples and reflectance measurements. A relationship between TSM concentration and reflectance was established for the range 400 – 900 nm. Data from Landsat TM, SPOT HRVIR and ASTER were calibrated and geometric corrected. The reflectance values were used to estimate the TSM concentration using the relationships established using the field measurements. The model coefficients and correlation factors, for identical bands on different sensors, presented a high similarity. The results have been incorporated in a Geographical Information System (GIS).

KEYWORDS: Remote Sensing, coastal zones, total suspended matter, breaking zone, geographical information system, empirical models.

1. INTRODUCTION

More than a half of the world's population live close to the sea. The coastal zone represents a comparatively small but highly productive and extremely diverse system, with a variety of ecosystems extending from coastal terrestrial to deep water regions approaching 200 m in depth [1]. The importance of understanding the land/ocean interaction, such as how changes on land may influence the biochemical and biophysical processes of the coastal seas, and vice versa, is fundamental to an assessment of the global implication of local changes in coastal seas [2].

Remote sensing techniques are a valuable tool to obtain specific information of the spatial and temporal characteristics of the coastal zone. Substances in surface water can significantly change the characteristics of surface water. Remote sensing techniques depend on the ability to measure these changes in the spectral signature backscattered from water and relate these measured changes by empirical or analytical models to a water quality parameter, such as suspended sediments [3]. Solar radiation reflected from sea water surfaces varies with the amount of suspended sediments and wavelength. In general, reflected solar radiation between wavelengths 500-700 nm increases as the concentration of suspended sediments increases [4].

The discrimination of suspended sediments or total suspended solids from water reflectance is based on the relationship between the scattering and absorption properties of water and its constituents. Most of the scattering is caused by suspended sediments and the absorption is controlled by chlorophyll-a and colored dissolved organic matter. These absorptives in-water components have been shown to lower the reflectance in a substantial way. However, this absorptives effects are generally in wavelengths less than 500 nm [5]. Therefore, we will concentrate on the visible and near-infrared (NIR) electromagnetic spectrum region to study the concentration of Total Suspended Matter (TSM). The spatial variation in the concentration of TSM in near coastal areas or estuaries can be quite difficult to describe, due to the effects of tides, coastal currents and waves [6].

Several studies have been done combining in situ measurements and satellite images in order to relate the water reflectance and the concentration of TSM. Ritchie et al. [7] developed an empirical approach to estimate the amount of TSM using water reflectance measured by remote sensing techniques. The general models of these empirical relations have the form of equation (1) or equation (2):

$$Y=AX+B \quad (1)$$

or

$$Y=AB^X \quad (2)$$

where X is the TSM concentration and Y is the water leaving reflectance. A and B are empirically derived factors. Islam et al. [8], Forget and Ouillon [9], Doraxan et al. [10] established empirical relationships (linear, polynomial, logarithmic, etc.) between remote sensing reflectance and TSM concentration. However, it has been showed in all of these studies that it is not possible to produce a single remote sensing algorithm to estimate the concentration and spatial variation of TSM with global validity, because of the influence on reflectance of the local conditions (particles size and density). Moreover, these studies were done for a fixed time and place and do not attempt to estimate these relations for different conditions. This issue becomes more difficult when we try to study a high dynamic area such as the sea breaking zone.

2. PROJECT STRATEGY

The main objective of this work was to evaluate the applicability of multi-spectral satellite images for coastal protection studies, particularly in the quantification of the TSM concentration in sea wave breaking zone.

2.1. Study area

A part of the Northwest coast of Portugal, centered in Aveiro, was chosen as a test area (Fig. 1). The total extension of this area is about 80 km. It is limited to the North by the Douro River mouth and to the South by the Mira Lagoon.

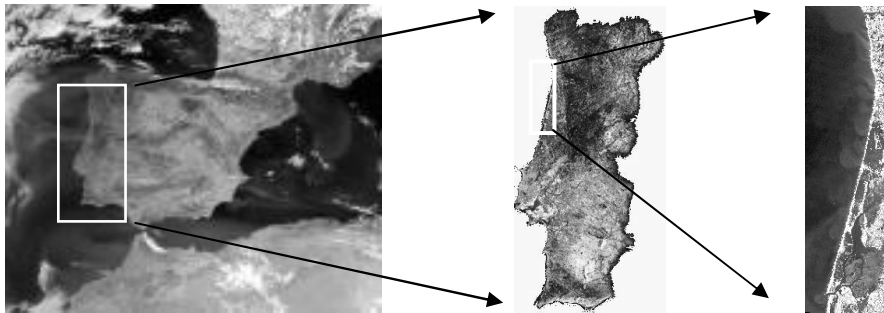


Fig. 1: Location of the study area about 80 km of coast centered in Aveiro

The littoral drift is the principal agent for the longshore sedimentary transport. In the Northwest coast of Portugal this current acts predominantly in the North-South direction.

The study area was chosen because presented a situation of generalized coastal erosion, in the last years. The causes of the present erosion in this particularly area have been identified as a coastal response to the weakening of the river basin sediment sources and river sediment transport, the mean sea level rise, the human occupation of waterfront and dune destruction [11]. The hydroelectric plants reduce drastically the volume of solids transported to the sea. The reduction of sediment transport is also associated to the extraction and dredging of sand rivers and to the river flow evolution along the year. The wave climate has medium significance with wave heights from 2 to 3 meters. Tides are of semidiurnal type, reaching a range of 2 to 4 meters for spring tides. Meteorological tides are not significant.

2.2. Initial approach

A number of aerial photographic surveys (1:8000) have been carried out, with cartographic objectives, covering the coast of continental Portugal. It is possible to discriminate areas with different sediment concentrations by visual inspection. However, there are obvious advantages in replacing the aerial surveys for satellite images. A single satellite image covers

a much larger area than a aerial photography, more frequently and at a lower cost. A first inspection of enhanced RGB colour composites of an ASTER satellite image with visible (green and red) and NIR bands showed that the same sort of patterns identified on the airphotos could also be identified on the satellite image. This is illustrated in Fig. 2.

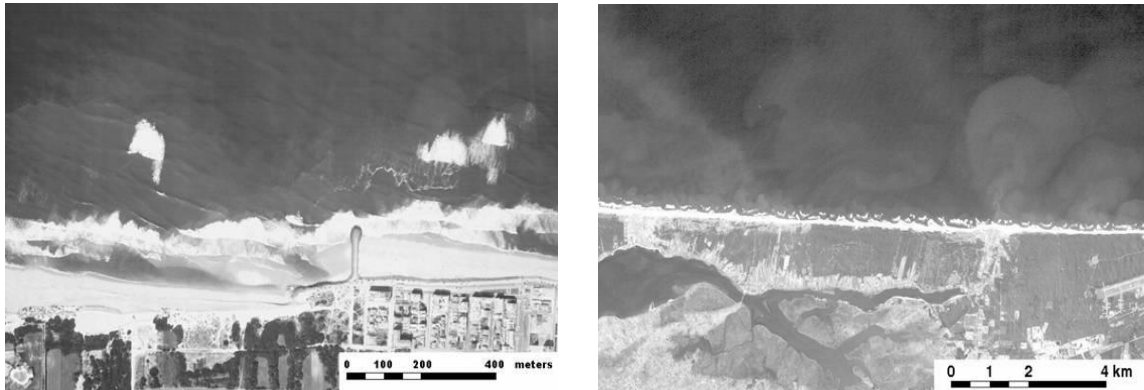


Fig. 2: Sedimentary patterns identified on an airphoto and on an ASTER image

Images of different sensors have been tested to select the most adequate for the discrimination of different sedimentary patterns. The sensors with the most adequate spectral, temporal and spatial resolution for the discrimination of zones with different concentrations of sediments are listed in table 1.

Table 1: Main characteristics of the satellite sensors used

| Satellite Sensor | Spectral Resolution | No. Bands | Spatial Resolution | Temporal Resolution |
|------------------|---------------------|-----------|--------------------|---------------------|
| Landsat TM | 30 (120) m | 7 | 450 – 1250 nm | ~ 2 weeks |
| SPOT HRVIR | 20/10 m | 4 | 500 – 1750 nm | ~ 2 weeks |
| TERRA ASTER | 15 (30 and 90) m | 14 | 400 – 1440 nm | ~ 2 weeks |

2.3. Data acquisition

A set of satellite images were acquired, five from Landsat TM, two from ASTER and one from SPOT HRVIR. These images are all cloud free. The image acquisition date and the corresponding time and tide height are presented in table 2.

Table 2: Acquisition parameters of the images used

| Satellite Sensor | Date | Acquisition Time | Tide Height (m) |
|------------------|-----------------|------------------|-----------------|
| Landsat TM | 9 November 1989 | 10:45 | 2.95 |
| Landsat TM | 4 May 1990 | 10:45 | 2.33 |
| Landsat TM | 1 November 1992 | 10:45 | 1.85 |
| Landsat TM | 13 June 1993 | 10:45 | 2.47 |
| Landsat TM | 24 July 1997 | 10:45 | 1.09 |
| SPOT HRVIR | 14 October 1998 | 11:35 | 2.85 |
| TERRA ASTER | 8 October 2001 | 11:43 | 1.29 |
| TERRA ASTER | 24 October 2001 | 11:43 | 2.07 |

3. METHODOLOGY

The methodology used in this study involved image processing for calibration satellite digital numbers (DN's) in reflectance values and geometric corrections. It also involved field data extraction and establishment of empirical models.

Different methods (maritime platforms, aerial platforms, simulation on the beach and water samples collection in the breaking zone) were used to determinate a relationship between the TSM concentration and the spectral response of the seawater.

3.1. Image Processing

All satellite image bands were calibrated for radiance values, using equation (3):

$$L_i = \alpha_i DN_i + \beta_i \quad (3)$$

where L_i is the spectral radiance ($Wm^{-2} sr^{-1} \mu m^{-1}$), DN_i is the digital number, α_i and β_i are the calibration coefficients for the spectral band i of a given sensor. The calibration coefficients used for ASTER images are listed in table 3.

Table 3: Radiance calibration coefficients for ASTER VNIR bands

| Band | Wavelength (nm) | Slope (α) | Offset (β) |
|------|-----------------|--------------------|--------------------|
| 1 | 520 - 600 | 0.676000 | -0.676000 |
| 2 | 630 - 690 | 0.708000 | -0.708000 |
| 3 | 760 - 800 | 0.862000 | -0.862000 |

The reflectance (R_i) values for all satellite image bands were obtained using the equation (4):

$$R_i = \frac{\pi L_i d^2}{E_i \cos \theta} \quad (4)$$

where L_i is the spectral radiance and E is the mean solar exoatmospheric irradiances for the spectral band i ; d is the Earth-Sun distance in astronomical units and θ is the solar zenith angle in degrees.

The ASTER and SPOT HRVIR geometric correction was made using Control Points (CP's) provided in the image header and further adjusted with Ground Control Points (GCP's). A total of 11 GCP's were collected with Global Positioning System receiver (GPS) and identified on each image. These points were reasonably well distributed around the interest area. The TM images were geometrically corrected using only an empirical transformation function obtained from the GCP's. The accuracy of the geometric correction was evaluated by a visual inspection on selected sites, such as airfields, crossroads and groins. The maximum error was about 1 pixel (or less) for all images used.

3.2. Field work

A crucial step in the quantitative use of remote sensing techniques is the *in situ* validation. For this particular application, it can be achieved by collecting water samples and measuring the water leaving reflectance. The "ground truth" data used in this study were obtained by boat, helicopter and water samples collection in the breaking zone. Several simulations were also made on different beaches of the study area in order to evaluate a large range of TSM concentrations.

A FieldSpec FR spectroradiometer was used, in all cases, to determinate the seawater reflectance. This optical sensor operates between the 350 nm and the 2500 nm and has 10 nm of spectral resolution. The data collection is made through a fiber optic cable input with 1.2 meters in length and a 25° full angle cone field-of-view. The data quality depends critically on the precision at the calibration stage. Based on the responsivity of the FieldSpec FR spectroradiometer, maximum radiance values measurable by the FieldSpec FR are well in excess of twice those for a 0° solar zenith angle and a 100% reflectance Lambertian panel [12].

The quantification of the TSM (mg/l) of the samples collected was made through a filtering process. The 1000 ml water samples collected were refrigerated in the dark and processed after a few hours in the chemistry laboratory. A cellulose nitrate filter was used, with a diameter pore of 0.45 μm . The filtering process comprises the following steps: (i) weigh and catalogue the filters; (ii) divide the water samples and filter; (iii) evaporation of the water contained in each filter; (iv) drying the filters and (v) weigh once again the filters. The quantification of TSM is made subtracting the final and initial weigh of the filters.

3.2.1. Maritime Platform

Three campaigns were carried out using boats of different types. The purpose of the field campaigns was to simultaneously collect water samples and measure the seawater leaving reflectance. The first two campaigns were scheduled so that they would coincide with clear-sky satellite overpasses by ASTER. The first attempt was in 11 October 2002, but the atmospheric conditions did not permit a satellite image acquisition. The second attempt was programmed for 24 June 2003, but unfortunately atmospheric conditions once again invalidated the image acquisition.

The subsequent field campaigns were carried out without any attempts to obtain a simultaneous image. A boat from the Portuguese Marine Institute was used in the 10 July 2003 to collect water samples and simultaneously measure the reflectance, as shown in Fig. 3 (a). The position and depth of each location was also measured using a GPS receiver and an echo-sounding lead. The main problems with this method was the difficulty to immobilize the boat and the impossibility to collect data close to the breaking zone.



Fig. 3: (a) Maritime Platform (b) Aerial Platform (c) Simulations (d) Water samples collection in the breaking zone

3.2.2. Aerial Platform

Helicopters provide an efficient platform for the collection of water samples and for reflectance measurements for several reasons. Firstly we can sample a large area rapidly, secondly we can immobilize the platform for making measurements, thirdly we can operate over specific areas in the sea breaking zone.

The helicopter was stabilized about 2-3 meters above the sea surface and 30 samples of water were collected and the reflectance measured simultaneously. The position of the helicopter was identified using a GPS. This method was the only one that allowed measurements to be made over the sea breaking zone. Fig. 3 (b) shows the helicopter used.

3.2.3. Simulations on the beach

Several field campaigns were carried out in different beaches to simulate different concentrations of suspended sediments and different types of sand (texture, colour and grain size). The sediment type was found to be very similar in the whole study area. A container with 80 cm of height and 40 cm diameter was used. To minimize the effect of reflection from the sides and bottom of the container, it was lined with a black and completely opaque plastic. The reflectance was measured and water samples were taken simultaneously, for a range of sediment concentrations (Fig.3 (c)).

The container conditions originated a signal attenuation in the reflectance values. This attenuation was quantified through some measures of the seawater samples reflectance carried out inside the container and also with a wet sand background. The relationship between container and wet sand background was found to be nearly constant for all concentrations of TSM tested. Fig. 4 (a) shows a typical example of this attenuation, in this case for a TSM concentration of 30 mg/l.

3.2.4. Water samples collection in the breaking zone

To get water samples directly from the breaking zone and the swash zone, a surfer went there and collected water samples in small containers (about 1000 ml), as shows Fig. 3 (d). The reflectance was measured for each water sample collected by putting the small container in the wet sand to try simulate the sea bottom conditions.

The average values of TSM concentration found in the breaking zone was 32 mg/l and in the swash zone 50 mg/l. The average reflectance values for these two areas are very similar, as it is shown in Fig. 4 (b).

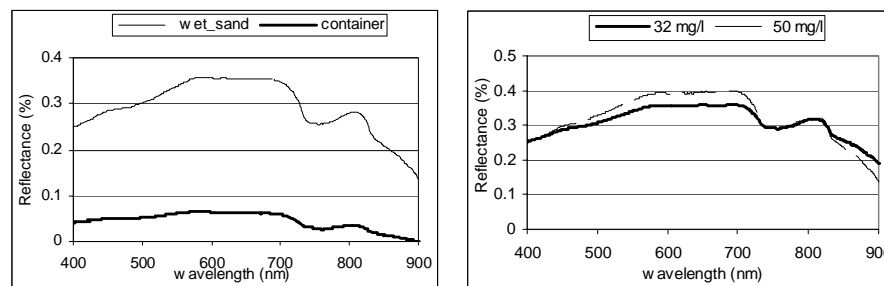


Fig. 4: (a) Attenuation factor (b) TSM concentration for two water samples collected in the breaking zone

3.3. Empirical models

The water leaving equivalent reflectance for each sensors band in the visible and NIR (R_{ES}) was calculated by equation (5), where R_m is the reflectance measured by the spectroradiometer, ϕ is the sensor spectral normalized response and λ is the wavelength.

$$R_{ES} = \frac{\int R_m(\lambda) \phi(\lambda) d\lambda}{\int \phi(\lambda) d\lambda} \quad (5)$$

A relationship between seawater reflectance and the TSM concentration was established for each band. Equations of linear models ($R=ATSM+B$), polynomial ($R=ATSM^2+BTSM+C$), logarithmic ($R=A\log_{10}(TSM)+B$), power ($R=ATSM^B$) and exponential ($R=Ae^{BTSM}$) models were tested for all satellite image bands. The coefficients of determination (R^2) were also determined for each model. For the visible and NIR bands of Landsat TM the linear and polynomial models tested presented a high determination coefficient ($R^2 \geq 0.96$). The results were a little bit worst for power and exponential models, as presented in table 4.

Table 4: Regression coefficients of reflectance functions vs TSM for TM data

| Bands | Linear | | | Polynomial | | | | Power | | | Exponential | | |
|-------|--------|-------|----------------|------------------|------|-------|----------------|------------------|------|----------------|-------------|------|----------------|
| | A | B | R ² | A | B | C | R ² | A | B | R ² | A | B | R ² |
| TM1 | 0.02 | 0.37 | 0.96 | 6E ⁻⁶ | 0.02 | 0.53 | 0.96 | 0.07 | 0.76 | 0.92 | 0.97 | 0.01 | 0.84 |
| TM2 | 0.03 | 0.09 | 0.97 | 1E ⁻⁶ | 0.03 | -0.12 | 0.97 | 0.04 | 0.93 | 0.94 | 0.90 | 0.01 | 0.82 |
| TM3 | 0.03 | -0.13 | 0.97 | 3E ⁻⁷ | 0.03 | 0.12 | 0.97 | 0.02 | 1.05 | 0.94 | 0.71 | 0.01 | 0.79 |
| TM4 | 0.02 | -0.63 | 0.96 | 1E ⁻⁵ | 0.01 | -0.28 | 0.97 | 5E ⁻⁴ | 1.62 | 0.90 | 0.12 | 0.01 | 0.70 |

The results obtained for SPOT HRVIR for all models tested are comparable to those obtained with TM data. As an illustration of the results obtained for SPOT HRVIR, Fig. 5 shows a graphical representation of the linear model for XS1, the polynomial model for XS2 and the power model for XS3.

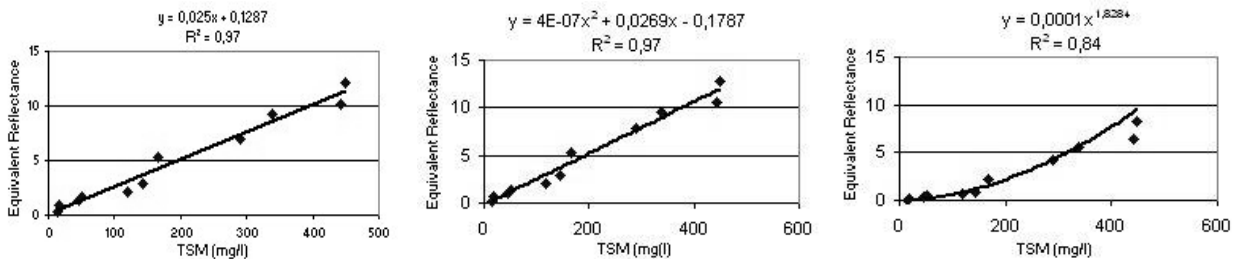


Fig. 5: Some empirical models for reflectance functions vs TSM for SPOT HRVIR

The coefficient of determination for all models established for ASTER VNIR bands are of the same sort as those obtained with SPOT HRVIR and TM data.

Table 5: Regression coefficients and correlation factor for reflectance functions vs TSM in the red bands, using a linear model

| Sensor/Band | Wavelength (nm) | A | B | R ² |
|-------------|-----------------|-------|-------|----------------|
| SPOT/XS1 | 500-590 | 0.025 | 0.128 | 0.97 |
| ASTER/VNIR1 | 520-600 | 0.025 | 0.131 | 0.97 |
| Landsat/TM2 | 520-600 | 0.026 | 0.088 | 0.97 |

The linear models established for all the images tested presents a determination factor (R^2) higher than 0.95. The non-linear models present a lower but acceptable coefficient of determination factor. A great similarity was verified between the model coefficients and determination factors, for spectrally comparable bands on different sensors. These parameters are presented in table 5 for the red bands of ASTER, TM and HRVIR.

4. CONCLUSIONS AND PLANS FOR FUTURE WORK

This study shows that multi-spectral satellite images can be used to obtain the TSM concentration in the sea breaking zone. However, the *in situ* measurements are essential to calibrate the process in order to establish the empirical relationships between TSM and water leaving reflectance.

The reflectance of all bands of the satellite images tested had very high correlation with the TSM in the wavelength between 500 and 900 nm. There is a peak in reflectance between 550 and 600 nm, and above 900 nm the reflectance is practically null (Fig. 6 (a)).

The great similarity observed between the model coefficients and determination factor, for identical bands of different sensors indicates a high confidence level in the established models.

The measurement conditions affect the results. The influence of sea bottom and the open ocean in the reflectance measures and the distribution of the sediments in the water column needs to be considered. The different measurement conditions carried out tried to address this issue. The container aimed to simulate the deep sea conditions, without the sea bottom influence, and the measures made with the wet sand background attempted to simulate the sea bottom influence.

A Geographic Information System (GIS) was developed, with all available information for the study area, including all available cartography and geographic databases. Information about TSM obtained from the boat and helicopter field campaigns is also being included. Specific tools are being developed for the GIS in order to properly address the physical processes in the coastal zone as a function of time.

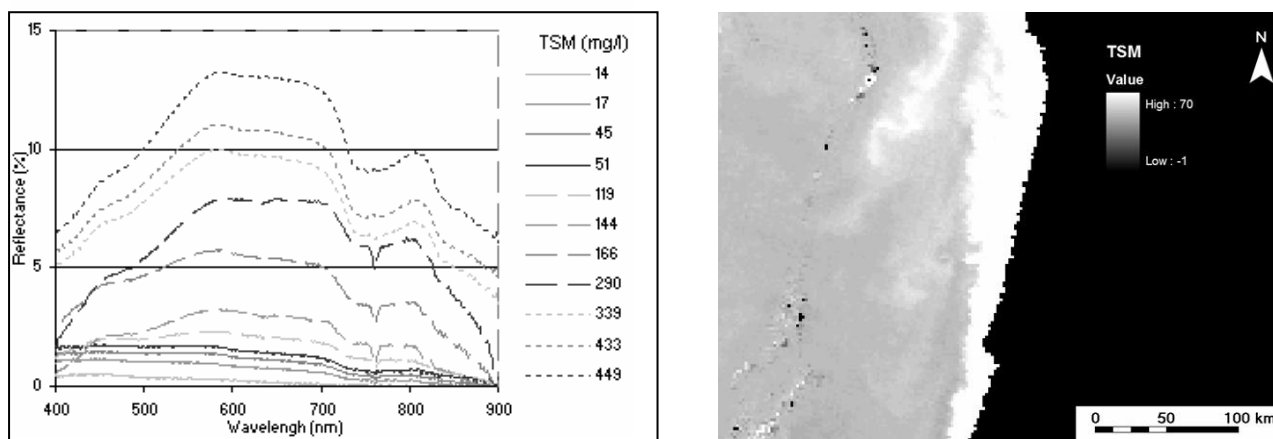


Fig. 6: (a) Relationship between TSM and seawater reflectance (b) MODIS image with TSM concentration

The atmospheric correction procedure is being implemented and is based on a simplified use of the 6S (Second Simulation of the Satellite Signal in the Solar Spectrum) radiative transfer code. A test of the method performance was already done by identifying areas that are expected to have a reasonably stable reflectance: sand areas and deep sea water (very low reflectance in NIR).

Work is currently being done in order to incorporate low spatial resolution satellite data from MERIS e MODIS in the GIS. These sensors provide nearly daily TSM images (Fig. 6 (b)), which could provide valuable additional information for coastal zone monitoring purposes.

ACKNOWLEDGEMENTS

This work was done within the COSAT project, financed by the Portuguese Science and Technology Foundation (FCT) through the POCTI/FEDER program.

The authors would like to thank the Instituto de Meteorologia, Alexandra Nunes and Prof. Rui Boaventura for they technical support and Janete Borges, Paulo Renato, Sónia Rey, Marlene Antunes and César Almeida for they assistance in the field work campaigns.

REFERENCES

1. Malthus, T.J., Mumby, P.J., Remote Sensing of the Coastal Zone:an Overview and priorities for Future Research, *International Journal of Remote Sensing*, Vol. 24, No.13, 2805-2815, 2003.
2. Vaughan, R., Sensing the Coastal Zones Remotely, *European Association of Remote Sensing Laboratories (EARSeL) Advances in Remote Sensing*, Vol. 4, No. 1-IX, 1995.
3. Ritchie, J.C., Zimba, P.V., Everitt, J.H., Remote sensing Techniques to Acess Water Quality, *Photogrammetric Engineering & Remote Sensing*, Vol. 69, N.º 6, pp. 695-704, 2003.
4. Muralikrishna, I.V., Remore Sensing Applications in Marine Science and Technology, 317-322, 1983.
5. Myint, S. W., Walker, N. D., Quantification of suspend sediments from satellite, *International Journal of Remote Sensing*, Vol. 23, No.16, pp. 3219-3249, 2002.
6. Mikkelsen, O.A., Examples of spatial and temporal variations of some fine-granied suspend oarticle characteristics in two Danish coastal water bodies, *Oceanologica Acta*, No. 25, 39-49, 2002.
7. Ritchie, J.C., McHenry, J.R., Schiebe, F.R., Wilson, R.B., The relationship of refelcted solar radiation and the concentration of sediment in the surfece water of reservoirs, *Remote Sensing of Earth Resources*, Vol. III, pp. 57-72, 1974.
8. Islam, M. R., Begun, S. F., Yamaguchi, Y., Ogawa, K., Suspend sediments in the the Ganges and Brahmaputra Rivers in Bangladesh: Observation from TM and AVHRR data, *Hydrological Processes*, Vol. 15, pp. 493-509, 2001.
9. Forget, P., Ouillon, S., Surface suspend matter off the Rhone river mouth from visible satellite imagery, *Oceanologica Acta*, Volume 21, n.º 6, pp. 739-749, 1998.
10. Doxaran, D., Froidefond, J. M., Lavender, S., Castaing, P., Spectral Signature of Highly Turbid Waters Application with SPOT Data to Quantify Suspend Particulate Matter Concentrations, *Remote Sensing of Environment*, No. 81, pp. 149-161, 2002.
11. Veloso-Gomes, F., Taveira-Pinto, F., Barbosa, J.P., Neves, L., Coelho, C., High risk situation in the NW Portuguese coast: Douro River – Cape Mondego, *Proceedings of Littoral 2002, The Changing Coast, EUROCOAST/EUCC*, Porto-Portugal, Ed. EUROCOAST – Portugal, pp. 411-421, ISBN 972-8558-09-0, 2002.
12. Analytical Spectral Devices, Inc., <http://www.asdi.com>, 2004

* amteodor@fc.up.pt; phone 00351 220100874; fax 00351 220100809; www.fc.up.pt